

Synthesis of BCN Ceramics from Pyrrolidine–Borane Complex

Yusuke Goto,^{a*} Makoto Sasaki,^b Masataka Hashizume^a and Masaaki Suzuki^c

^aDivision of Chemical and Materials Engineering, Faculty of Engineering, Muroran Institute of Technology, 27-1 Mizumoto, Muroran, Hokkaido 050-8585, Japan

^bDepartment of Material Science and Engineering, Faculty of Engineering, Muroran Institute of Technology, 27-1 Mizumoto, Muroran, Hokkaido 050-8585, Japan

^cHokkaido National Industrial Research Institute Agency of Industrial Science and Technology, Ministry of International Trade and Industry, 2-17 Tsukisamu-Higashi, Toyohira, Sapporo, Hokkaido 062-0052, Japan

(Received 14 July 1998; accepted 6 February 1999)

Abstract

BCN ceramics were prepared from pyrrolidine–borane complex. Its complex was a new product and has not appeared on the market. The chemical compositions of the BCN ceramics were $BC_{1.5}N_{0.4}$ obtained at 1000°C in Ar, $BC_{0.9}N_{0.4}$ obtained at 1000°C in NH_3 . Boron was a mixture of trigonal and tetragonal B–N bonds. Electrical conductivity, of the BCN ceramics showed semiconductive properties. © 1999 Published by Elsevier Science Limited. All rights reserved

Keywords: BCN, turbostatic structures, precursors–organic, electrical conductivity.

1 Introduction

In synthesis methods of BCN ceramics the CVD method is widely used.^{1–4} However, bulk forming and large-scale preparation are difficult in this method. Bulk forming is necessary for evaluating various properties of BCN ceramics. Accordingly the precursor method has been focused on breaking through these problems.⁵ This method can be applicable for the preparation of ceramics from organic macromolecules as starting material. It is expected that the coordination number and chemical composition in the BCN ceramics could be controlled by dealing with starting materials. Bill *et al.* reported that BCN ceramics were prepared by this method from a pyridine–borane complex.^{6–8} Amorphous ceramics of BC_4N and BN composition were prepared at 1050°C in Ar and in NH_3 , respectively. Boron coordinations for both BC_4N and BN were trigonal and exist as B–N bonds in the ceramics. The heat-treated specimen in

Ar atmosphere showed semiconductive properties and the energy gap was 0.07 eV. The heat-treated specimen in NH_3 was an insulator. In the case of the piperazine–borane complex as a starting material, the composition was BC_2N at 1050°C in Ar and contained also trigonal B–N boron atoms identical with the pyridine–borane complex. But, the other heterocyclic compounds cannot be examined as starting materials because these starting materials are not available on a commercial basis. Therefore, the object of these works was to prepare a new pyrrolidine–borane complex from the reaction of pyrrolidine and a borane–dimethyl sulfide complex as a first stage. In this study, the authors have attempted to investigate the structural correlation between precursor and ceramics.

2 Experimental

2.1 Synthesis of a pyrrolidine–borane complex

Borane–dimethyl sulfide complex [0.1 mol (50 ml)] in 2 M toluene was dropped into 0.1 mol (10 ml) of pyrrolidine at 0°C in 0.1 MPa Ar and the solution was stirred for 24 h and cooled by using ethanol with dry ice. The toluene was removed and the pyrrolidine–borane complex was obtained as precipitation product.

2.2 Synthesis of a pyrrolidine–borane derivative (preceramic)

The pyrrolidine–borane complex obtained was heated at 100°C for 5 h in 0.1 MPa Ar, then at 200°C for 10 h, at 300°C for 24 h and at 400°C for a further 24 h continuously. The colorless and transparent liquid changed to a brown liquid, and then to a brown solid. The brown solid obtained was milled (<75 μm) and pyrrolidine–borane preceramic powder was prepared.

*To whom correspondence should be addressed.

2.3 Synthesis of BCN ceramics

The powdered pyrrolidine–borane preceramic was heated at 1000°C for 2 h (heating rate: 250°C h⁻¹) in Ar (purity: 99.99%) and NH₃ (purity: 99.9%) (flow rate: 0.5 l min⁻¹, 0.1 MPa). The specimen was washed by ethanol and a BCN ceramic was prepared.

2.4 Analysis

The analysis of the ceramics obtained was evaluated by TGA (Sinku-Riko TCD-9800A carrier gas: Ar, flow rate: 50 ml min⁻¹, heating rate: 250°C h⁻¹), gas chromatograph (Yanaco G3810TCD Column: Porapack N, carrier gas: He, flow rate: 50 ml min⁻¹), FT-IR (Jasco FT-IR 5300 type Fourier transforms infrared spectroscopy), ¹¹B solid state NMR (Jeol JNM-GX270), elemental analysis (N, O: Horiba Oxygen/Nitrogen analyzer 550, 650 series, C, S: Carbon/Sulfur analyzer 510, 511, 512) and X-ray diffraction (CuK_{α1}/40 KV/20 mA, 2θ = 10–80°).

3 Results and Discussion

3.1 The pyrrolidine–borane derivative (preceramic)

The FT-IR spectra of the pyrrolidine–borane complex and preceramic are shown in Fig. 1. N–H bonds (3180 cm⁻¹) and B–H bonds (2300 cm⁻¹) exist in the complex. However, both N–H and

B–H bonds in the preceramic disappeared by pyrolysis. The FT-IR spectra of h-BN, which has trigonal B–N bonds [defined as B(sp²)-N], and the c-BN, which has tetragonal B–N bonds [defined as B(sp³)-N] are also shown in Fig. 1. Trigonal and tetragonal B–N bonds exist in both the complex and preceramic. The absorption intensity of h-BN around 1390 cm⁻¹ is strong and c-BN is relatively very weak.^{3–9} The trigonal B–N bond absorption of the preceramics is weak as shown in Fig. 1. The tetragonal B–N bonds also exist in the preceramic, but it is hard to discuss a ratio of B(sp³)-N to B(sp²)-N by FT-IR results. The results of ¹¹B solid state NMR measurement are shown in Fig. 2. The preceramic shows a single symmetrical resonance the same as c-BN.¹⁰ Accordingly, trigonal B–N bonds the same as h-BN and tetragonal B–N bonds coexist in the preceramic as shown by FT-IR.

The molar chemical composition of the pyrrolidine–borane complex and the preceramic were B₁C₄N₁H₁₂ (calculated) and B_{1.0}C_{2.6}N_{0.2}H_{5.0}, respectively. The chemical composition of the pyridine–borane complex and the preceramic were B₁C₅N₁H₅ (calculated) and B_{1.0}C_{3.7}N_{0.9}H_{7.3}, respectively. The decrease of nitrogen in the pyrrolidine–borane preceramic was larger than that of the pyridine–borane preceramic. Pyrolysis of the pyrrolidine–borane preceramic may progress further

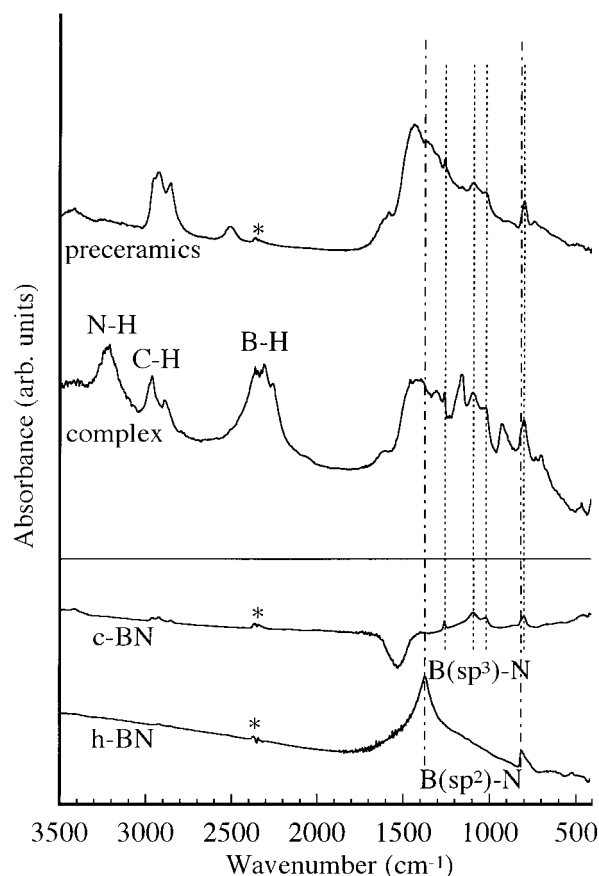


Fig. 1. FT-IR spectra of a pyrrolidine–borane complex, preceramics, c-BN and h-BN. B(sp²)-N: trigonal B–N bond; B(sp³)-N: tetragonal B–N bond; * CO₂.

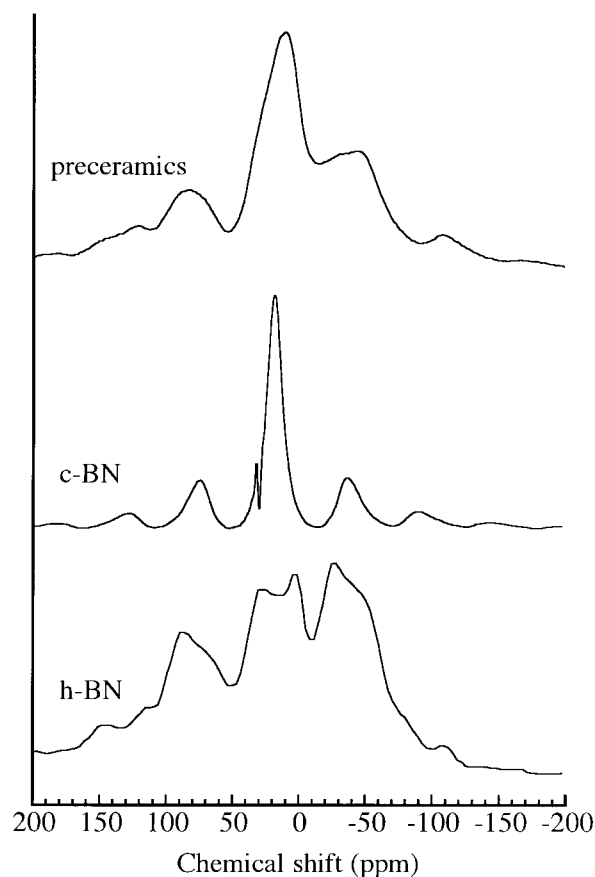


Fig. 2. ¹¹B solid state NMR spectra of pyrrolidine–borane preceramics, c-BN and h-BN.

because of no conjugated double bonds in the pyrrolidine–borane complex as starting material.

The bonds concerning hydrogen such as B–H, C–H and N–H decreased in the pyrrolidine–borane preceramic in comparison with the pyridine–borane preceramic. The chemical composition of the preceramic was $B_{1.0}C_{2.6}N_{0.2}H_{5.0}$.

3.2 BCN ceramics

Heat treatment of the pyrrolidine–borane preceramic was performed in Ar atmosphere and Fig. 3 shows the thermogravimetric change during pyrolysis. The y1 axis shows the thermo gravimetric change and the y2 axis shows the derivative curve of y1. The ceramic yield was about 60% by heat treatment up to 1000°C. The rapid weight decrease occurred around 400°C. Around this temperature, the pyrrolidine–borane preceramic gave off hydrocarbon (ethane and ethylene) gasses as detected by gas chromatograph. To determine a structural change of the pyrrolidine–borane preceramic, FT–IR and ^{11}B -NMR solid state NMR measurements were achieved. The FT–IR spectra of the BCN ceramic obtained in both Ar and NH_3 by heat treatment at 1000°C are shown in Fig. 4. The peaks are indistinct from the pyrrolidine–borane preceramic because of the broadening and decreasing of absorption. The existence of trigonal B–N bonds can be confirmed in comparison with around 1390 and 850 cm^{-1} of h-BN as standard. However, it is not clear whether tetragonal B–N bonds exist or not.

Therefore, ^{11}B solid state NMR spectra are demonstrated in Fig. 5. The splitted peaks at 0 and 30 ppm of the BCN ceramic prepared at

1000°C in both NH_3 and Ar can be assigned as trigonal B–N bonds. Considering the FT–IR (Fig. 4) and ^{11}B -NMR (Fig. 5), trigonal and tetragonal B–N bonds coexist, and trigonal B–N bonds of the ceramics increase with increasing heat

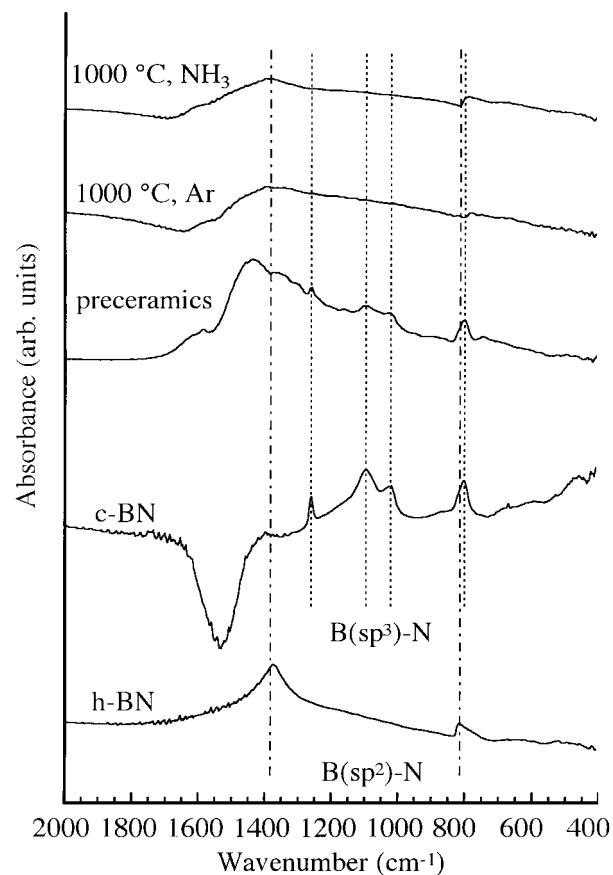


Fig. 4. FT–IR spectra of pyrrolidine–borane preceramics, BCN ceramics, c-BN and h-BN. $B(sp^2)$ -N :trigonal B–N bond; $B(sp^3)$ -N :Tetragonal B–N bond.

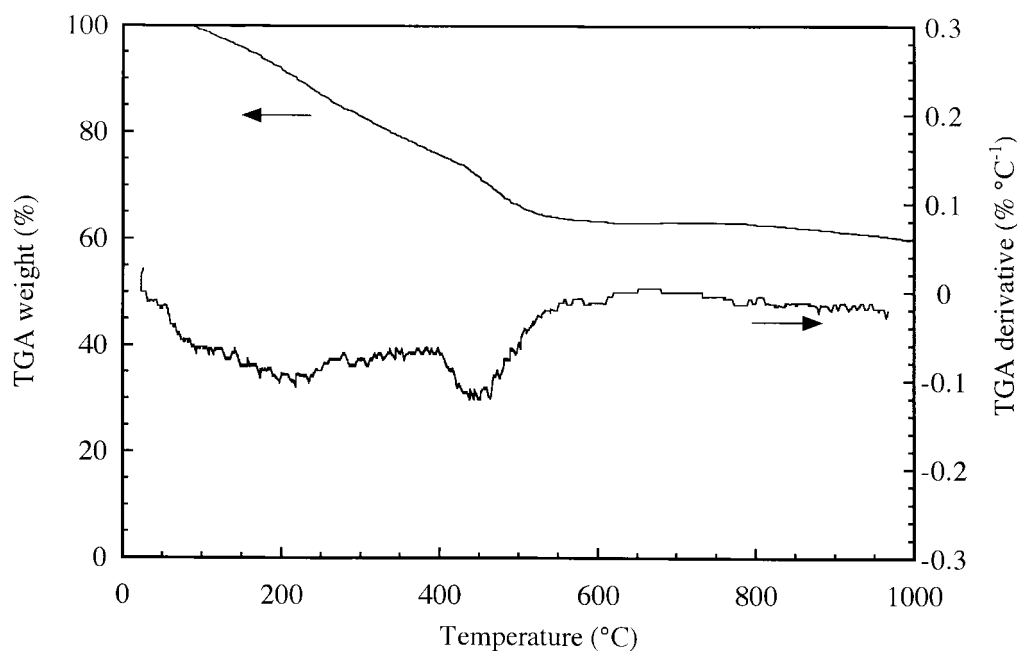


Fig. 3. TGA and its derivative curves of pyrrolidine–borane preceramics in Ar.

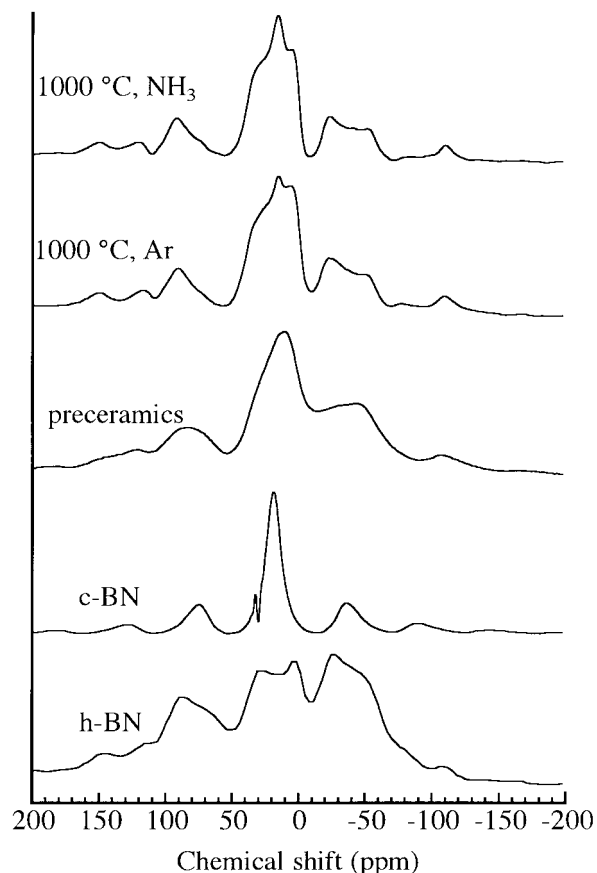


Fig. 5. ^{11}B solid state NMR spectra of pyrrolidine-borane preceramics, BCN ceramics. c-BN and h-BN.

treating temperature.^{10,11} It is thought to be due to the thermal stability of trigonal B–N bonds in the atmospheric pressure. On the other hand, the BCN ceramic derived from the pyridine-borane complex at the same temperature and in the same atmosphere were of trigonal B–N bonds only. The difference between the pyrrolidine-borane and a pyridine-borane-derived BCN ceramic maybe caused by the bond angle between a lone pair of the nitrogen and the basal plane of the heterocyclic compounds as shown in Fig. 6. In other words, pyridine has a lone pair of nitrogen in parallel to the facets of a six-member ring. Therefore, when borane coordinates at a lone pair of nitrogen, B–N bonds formed tend to orient in parallel with the facets, a plane structure of the BCN ceramic is kept and boron has a trigonal B–N structure even when the complex is heated at 1000°C. In the case of the pyrrolidine-borane complex, the bond angle between B–N and basal plane is less than 180° as shown by Fig. 6. Trigonal B–N bonds may not be completely stable because of the smaller bond angle of the pyrrolidine-borane complex. Therefore, co-existence of the trigonal and tetragonal B–N bonds may result from the smaller bond angle of the pyrrolidine-borane complex as a starting material.

The results of chemical composition analysis are shown in Table 1. As compared with the pyrroli-

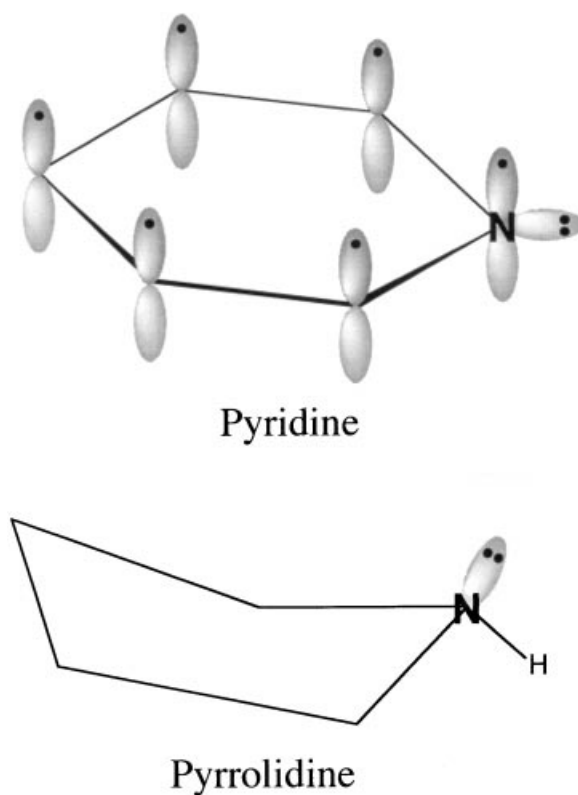


Fig. 6. Electron structures of heterocyclic compounds.

Table 1. Chemical composition of pyrrolidine-borane preceramics and BCN ceramics (molar ratio)

	B	C	N	H
Preceramics	1.0	2.6	0.17	5.6
1000°C, Ar	1.0	1.5	0.40	0.42
1000°C, NH ₃	1.0	0.90	0.40	0.66

dine-borane preceramic, the specimens heated at 1000°C in Ar and NH₃ atmospheres decreased in both carbon and hydrogen. This is due to the formation of hydrogen and hydrocarbon gas as described above. B/N ratio of the preceramic was smaller than the corresponding ratio of the BCN ceramic. A part of boron reacted with a very small amount of oxygen and B₂O₃ was formed. The measurement of the chemical analysis was performed after dissolving and removing of B₂O₃ by ethanol. Therefore, B/N ratio relatively increased. The reason for the higher amount of nitrogen in the ceramic is due to almost no NH₃ gas formation during 1000°C heating. As a result of the hydrocarbon gas and B₂O₃ formation, nitrogen content in the ceramic increased.

The results of X-ray diffraction are shown in Fig. 7. The typical halo patterns obtained show graphite-like turbostatic structures for 1000°C products. The patterns exhibit the (002) diffraction ($2\theta \approx 25^\circ$) characterized as interlayer spacing and the (100) diffraction ($2\theta \approx 25^\circ$). The graphite-like turbostatic structure of the pyrrolidine-borane-

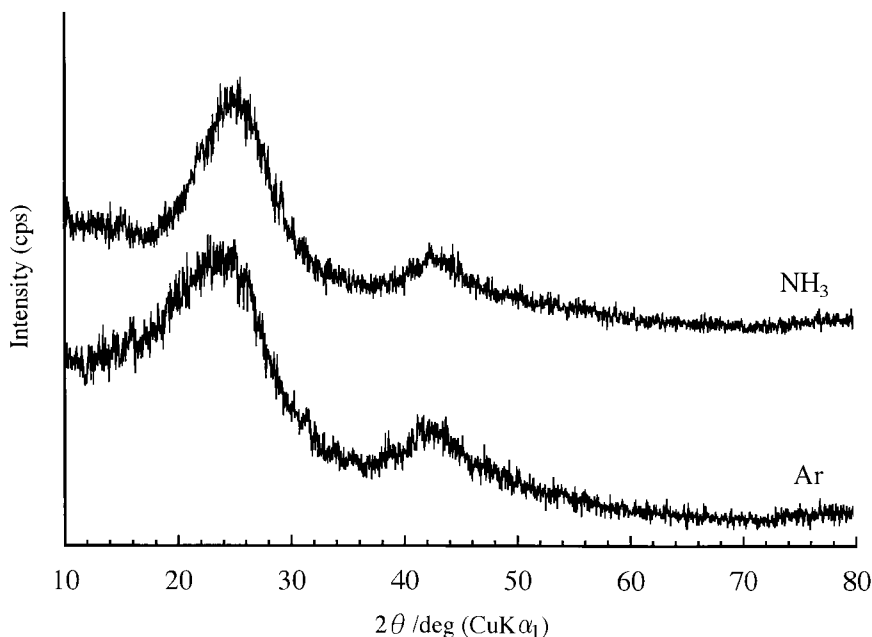


Fig. 7. X-ray diffraction patterns of BCN ceramics derived from pyrrolidine–borane preceramics at 1000°C in Ar and in NH₃.

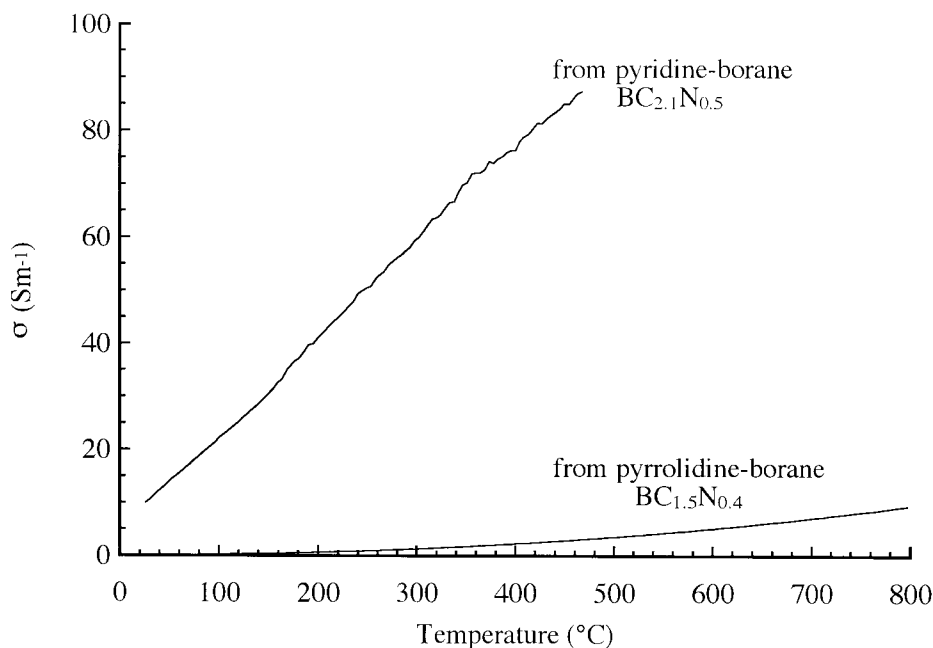


Fig. 8. Electrical conductivities of BCN ceramics prepared at 1000°C in Ar.

derived BCN ceramic is similar to other BCN ceramics obtained from corresponding heterocyclic compounds.

Figure 8 shows the electrical conductivities of BCN ceramics performed by a direct current two-terminal method, and also shown for comparison is the other BCN ceramic obtained by heat treatment at 1000°C in Ar from the pyridine–borane complex. Semiconductive property is shown to increase in both cases according to the rise in temperature. The difference in the electrical conductivity of both is because of the difference in carbon content. The orders of electrical conductivities

are not so high in comparison with graphite. The existence of B–N bonds may obstruct the conductivity by carbon network.

Mott's plots are well known to examine a conduction mechanism.^{12–14} Figure 9 shows Mott's plots for the two types of BCN ceramics. Hopping conduction is dominant to the BCN ceramic from the pyrrolidine–borane as by a minus straight line inclination. On the other hand, inclination is not a completely straight line in the case of BCN from the pyridine–borane. This is thought to be mainly because of the difference in carbon content as when a difference in conductivity appears. All six-member

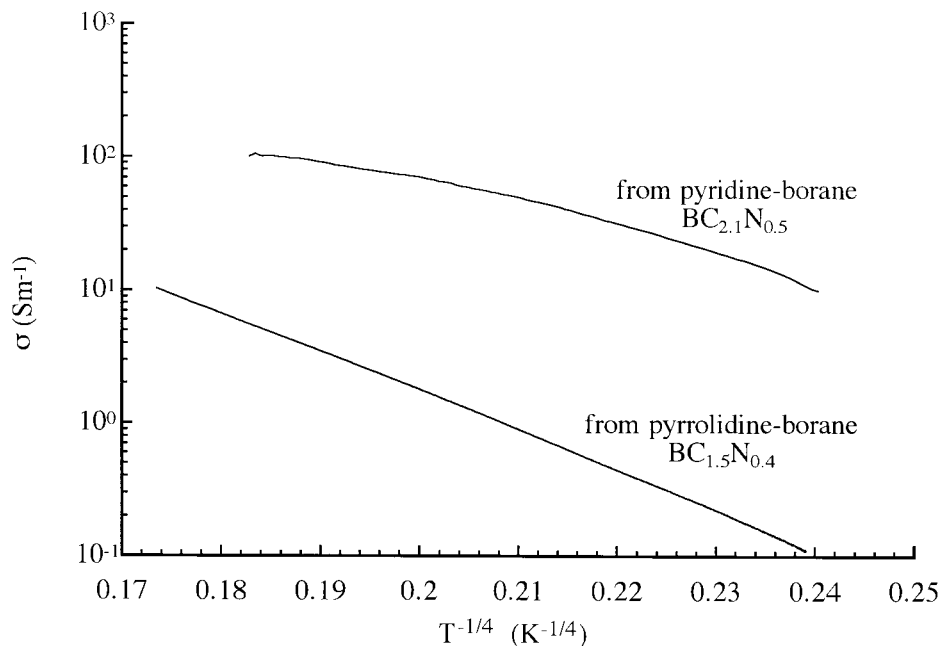


Fig. 9. Mott's plots of BCN ceramics prepared at 1000°C in Ar.

rings which consist of carbon in the parts caused by a relatively large amount of carbon like a BCN from the pyridine–borane complex may lead to higher conductivity by passing through at that point. However, boron and nitrogen atoms which act as impurities in conduction in the other parts may contribute to express a hopping conduction. The reason for a non-straight line of the WN ceramic from pyridine–borane is mentioned above. It is conjectured a hopping conduction of the BCN ceramic from pyrrolidine–borane is due to smaller carbon content than that from the pyridine–borane complex.

4 Conclusion

Turbostatic $BC_{1.5}N_{0.4}H_{0.42}$ and $BC_{0.9}N_{0.4}H_{0.66}$ ceramics were prepared from a pyrrolidine–borane complex at 1000°C in Ar and in NH_3 , respectively. Both BCN ceramics were graphite-like turbostatic structures which consist of trigonal and tetragonal B–N bonds.

Acknowledgements

The authors wish to thank Prof. Dr. S. Shimada for ^{11}B -NMR measurements, and thank Mr. T. Hoshi of Nittestu Cement Co. Ltd. for hydrogen and boron analysis.

This research was supported in part by the Grant-in-Aid for Scientific Research from the Ministry of Education, Science, Sports and Culture under contract Nos. 10137201, 09229203 and 08243203 and a Sasakawa Scientific Research Grant.

References

1. Saugnac, F., Teyssandier, F. and Marchand, A., Characterization of C–B–N solid solutions deposited from a gaseous phase between 900 and 1050°C. *J. Am. Ceram. Soc.*, 1992, **75**(1), 161–169.
2. Besmann, T. M., Chemical vapor deposition in the boron–carbon–nitrogen system. *J. Am. Ceram. Soc.*, 1990, **73**(82), 498–2501.
3. Yamada, M., Nakanishi, M. and Sugishima, K., Improvements of stress control ability and radiation resistance by adding carbon to boron. *J. Electrochem. Soc.* 1990, **137**(7) 2242–2246.
4. Komatsu, T., Kakudate, Y. and Fujiwara, S., Heat resistance of a shock-synthesized BCN heterodiamond. *J. Chem. Soc., Faraday Trans.*, 1996, **92**(24), 5067–6071.
5. Bill, J., Kienzle, A., Sasaki, M., Riedel, R. and Aldinger, F., Novel routes for the synthesis of materials in the quaternary system Si–B–C–N and their characterisation. In 8th CIMTEC, ed. P. Vincenzini. Elsevier Science Publishers B. V. in press.
6. Bill, J., Frieß, M. and Riedel, R., Conversion of amineboranes to boron carbide nitride. *Eur. J. Solid State Inorg. Chem.*, 1992, **29**, 195–212.
7. Bill, J., Riedel, R. and Passing, G., Amine-borane als precursoren für borcarbidinitrid. *Z. anorg. allg. Chem.*, 1992, **610**, 83–90.
8. Riedel, R., Bill, J. and Passing, G., A novel carbon material derived from pyridine–borane. *Adv. Mater.*, 1991, **3**(111), 551–552.
9. Geick, R. and Perry, C. H., Normal modes in hexagonal boron nitride. *Phys. Rev.*, 1996, **146**(2), 543–547.
10. Marchetti, P. S. Kwon, D. Schmidt, W. R., Interrante, L. V. and Maciel, G. E., High-field ^{11}B magic-angle spinning NMR characterization of boron nitrides. *Chem. Mater.*, 1991, **3**, 482–486.
11. Eaton, G. R., NMR of boron compounds. *Chem. Mater.*, 1969, **46**(9), 547–556.
12. Mott, N. F., Conduction in non-crystalline systems: I. localized electronic states in disordered systems. *Phil. Mag.*, 1968, **17**, 1259–1267.
13. Mott, N. F., Conduction in non-crystalline systems: II. the metal-insulator transition in a random array of centres. *Phil. Mag.*, 1968, **17**, 1268–1284.
14. Mott, N. F., Conduction in non-crystalline materials: III. localized states in a pseudogap and near extremities of conduction and valence bands. *Phil. Mag.*, 1969, **17**, 835–852.